Supplement of

Brief communication: Storstrømmen glacier, Northeast Greenland, primed for end-of-decade surge

Jonas K. Andersen[1], Rasmus P. Meyer[1], Flora S. Huiban[1], Mads L. Dømgaard[1], Romain Millan[2], and Anders A. Bjørk[1]

[1]Department of Geosciences and Natural Resource Management, University of Copenhagen, Copenhagen Denmark
[2]Univ. Grenoble Alpes, CNRS, IRD, INRAE, Grenoble-INP, IGE (UMR 5001), 38000 Grenoble, France

Correspondence: Jonas K. Andersen (joka@ign.ku.dk)

Supplementary Figures

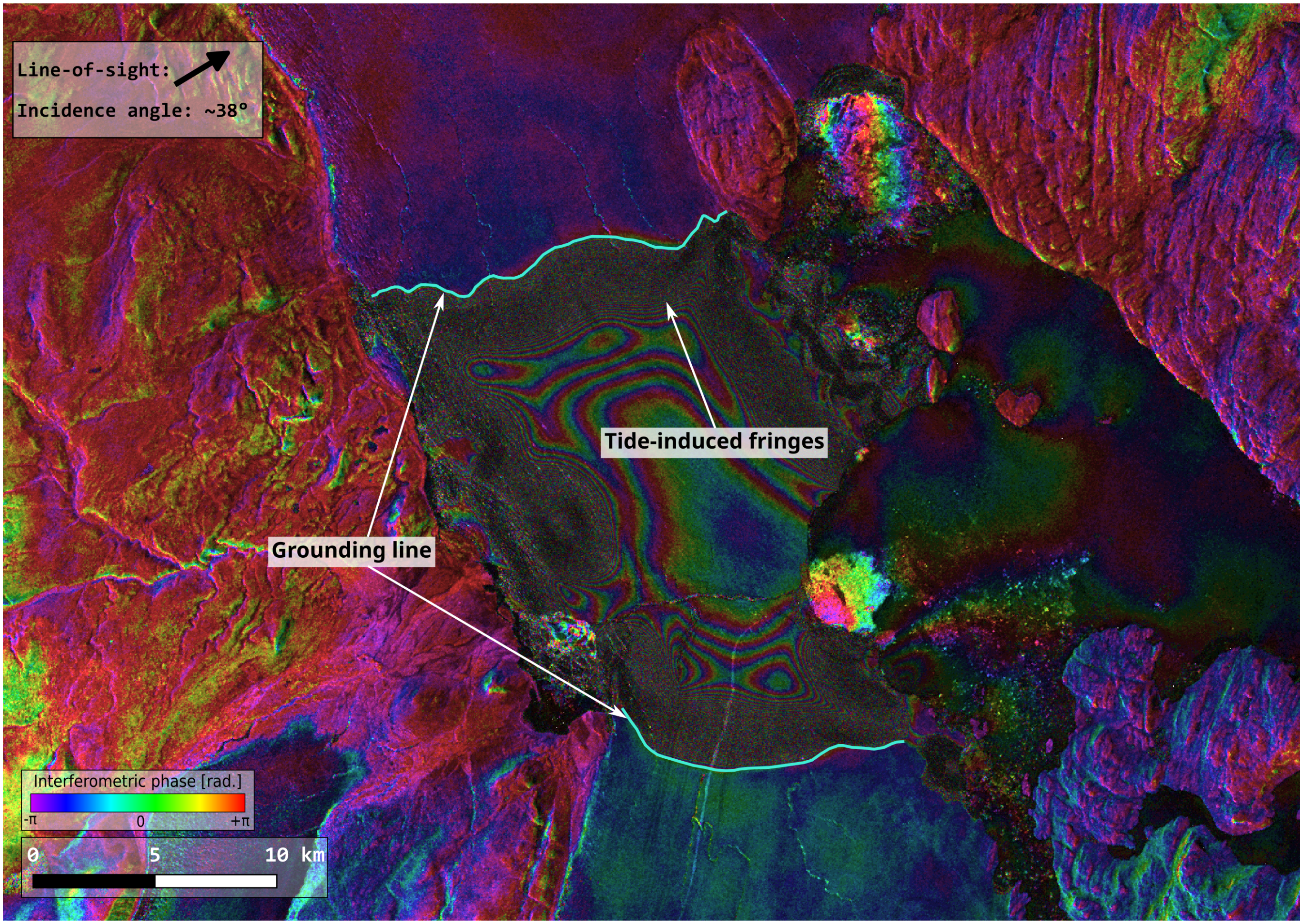

Figure S1. Sentinel-1 double-difference interferogram exemplifying the mapping of grounding lines for Storstrømmen (top) and L. Bistrup (bottom). The phase of the double-difference interferogram is sensitive to changes in the displacement field between the two interferograms (in this case spanning the temporal baselines 10th - 16th April 2018 and 16th - 22nd April 2018) in the radar line-of-sight, and a denser fringe pattern indicates a larger displacement change. Assuming no changes in horizontal ice flow between the two interferograms, the dense fringe pattern observed here is caused by a difference in the tide amplitude between the two interferograms, which leads to a difference in vertical uplift. The upstream limit of these tidally induced fringes is interpreted as a proxy for the glacier grounding line.

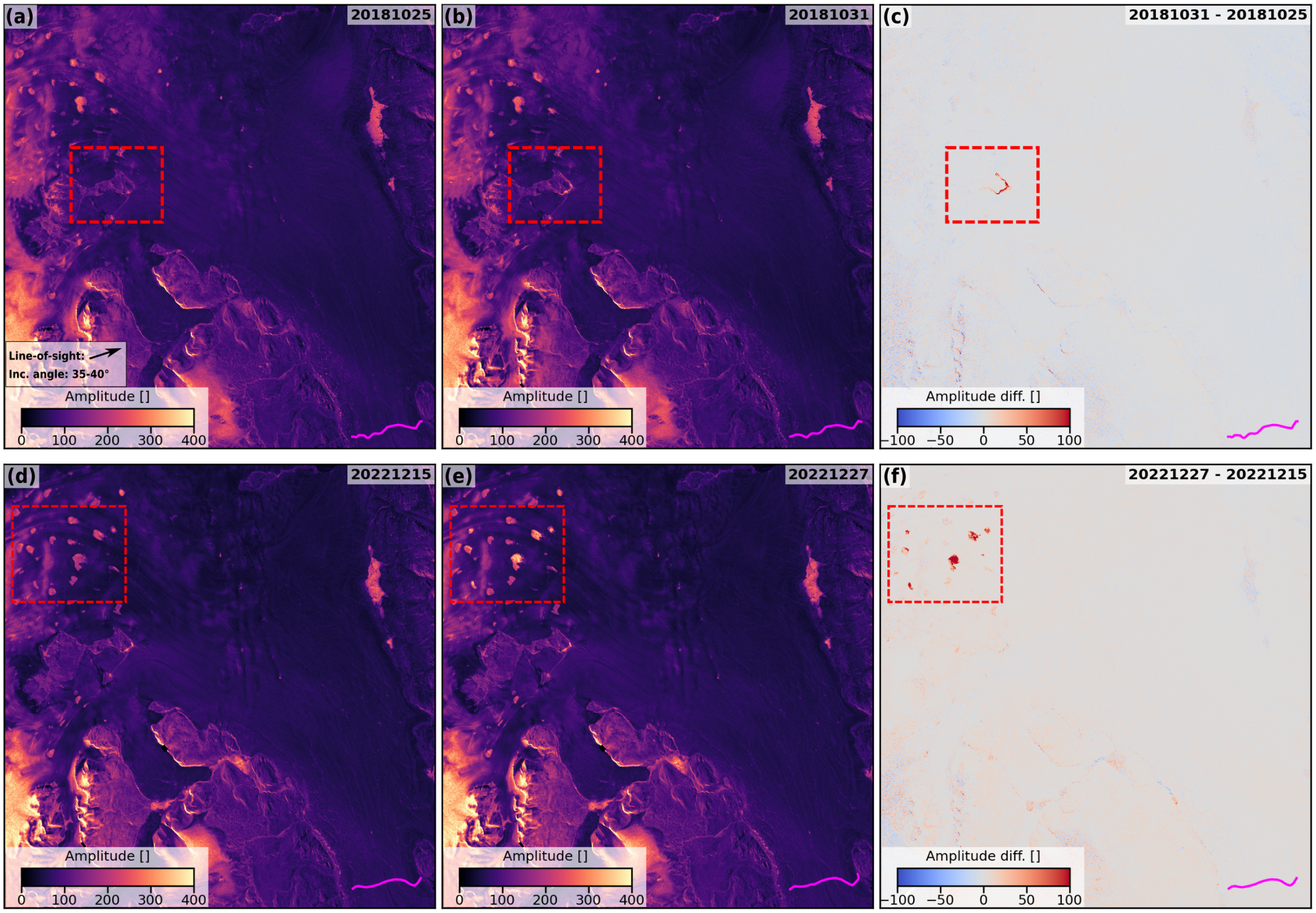

Figure S2. Sentinel-1 amplitude images revealing ice surface changes related to the transient dynamic events documented in Figure 3 in the main text. The imaged region is the same as in Figure 3. (a)-(b) Amplitude images from October 25th and 31st 2018 and (c) the amplitude difference between these acquisitions - an increase in amplitude is observed over an ice-dammed lake just upstream from where flow acceleration is observed (Figure 3 panels (a)-(c)), indicating a potential drainage of the lake. (d)-(e) Amplitude images from December 15th and 27th 2022 and (f) the difference between these acquisitions - amplitude increases are observed over multiple of the supraglacial lakes in this region, coinciding with the transient flow changes shown in Figure 3 panels (d)-(f), indicating that one or more of these lakes may have drained.

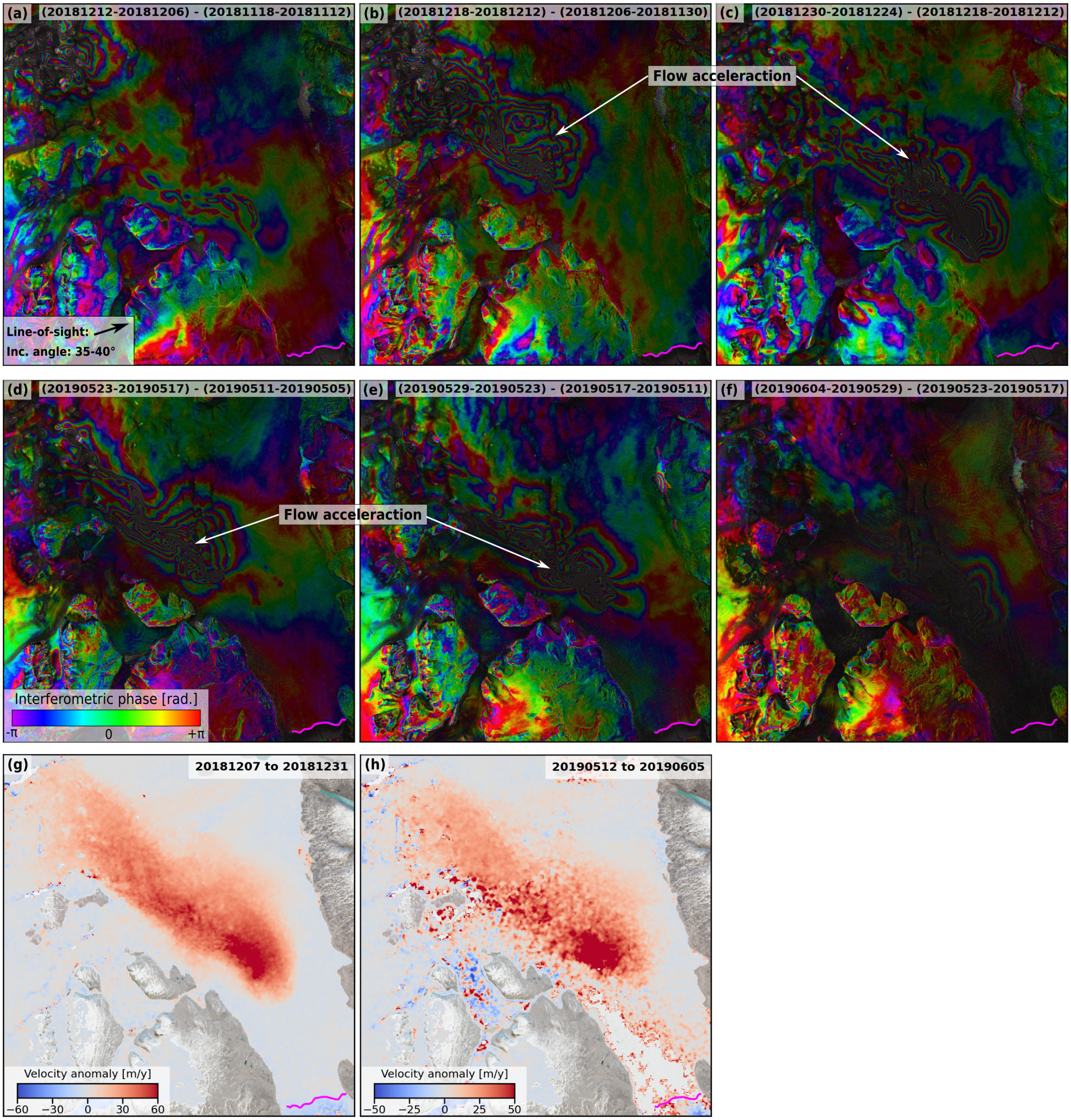

Figure S3. Sentinel-1 double-difference interferograms showing dynamical effects related to an apparent drainage event in upstream Storstrømmen during December 2018 (a)-(c) and May 2019 (d)-(f). The box in panel (a) indicates the ground-projected line-of-sight direction and incidence angle of Sentinel-1 track 74 (used for all the measurements in (a)-(f)). Panels (g) and (h) show PROMICE ice velocity magnitude anomalies for two 24-day periods spanning the identified events. The solid magenta line indicates the Storstrømmen grounding line.

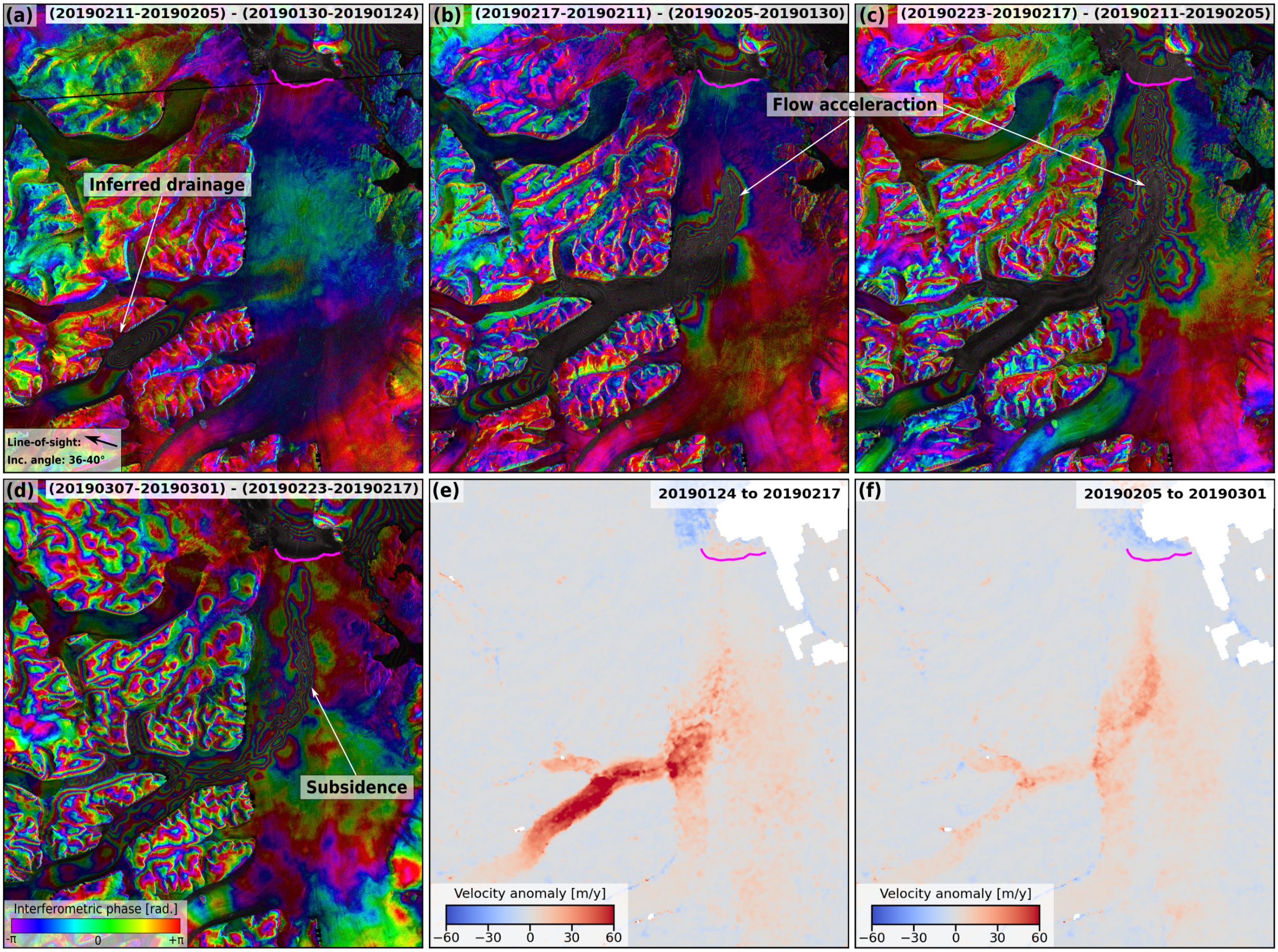

Figure S4. (a)-(d) Sentinel-1 double-difference interferograms showing dynamical effects related to an apparent drainage event upstream of L. Bistrup glacier during winter 2019. The box in panel (a) indicates the ground-projected line-of-sight direction and incidence angle of Sentinel-1 track 170 (used for all the measurements in (a)-(d)). Panels (e) and (f) show PROMICE ice velocity magnitude anomalies for two 24-day periods spanning the identified event. The solid magenta line indicates the L. Bistrup grounding line.

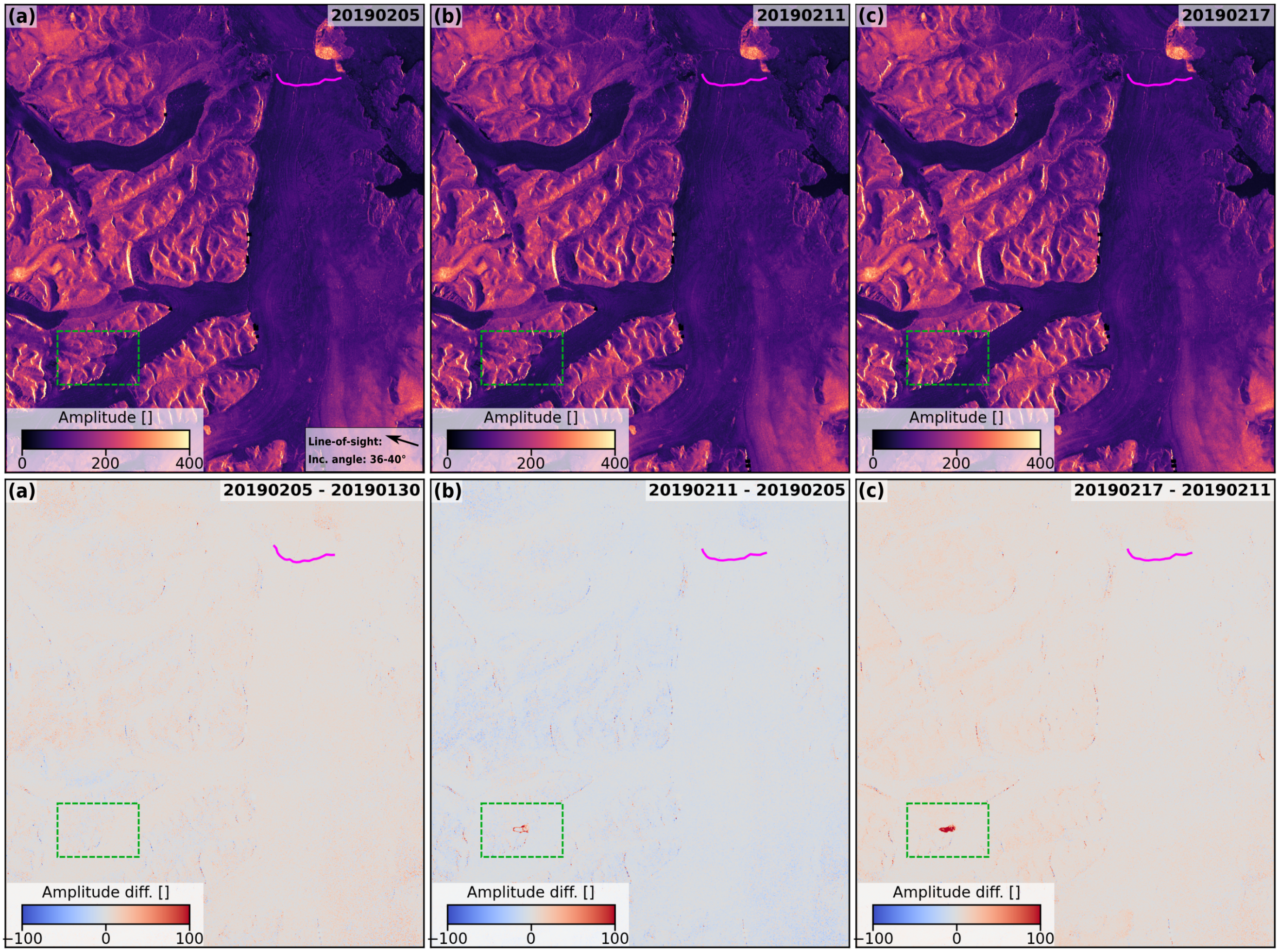

Figure S5. Sentinel-1 amplitude images revealing ice surface changes related to the transient dynamic events documented in Figure S4 above. (a)-(c) Amplitude images from February 5th, 11th, and 17th 2019. (d)-(f) Amplitude difference maps for these acquisitions - an increase in amplitude is observed over an ice-dammed lake just upstream from where flow acceleration is observed in Figure S4, suggesting a potential drainage of the lake (green dashed rectangle).

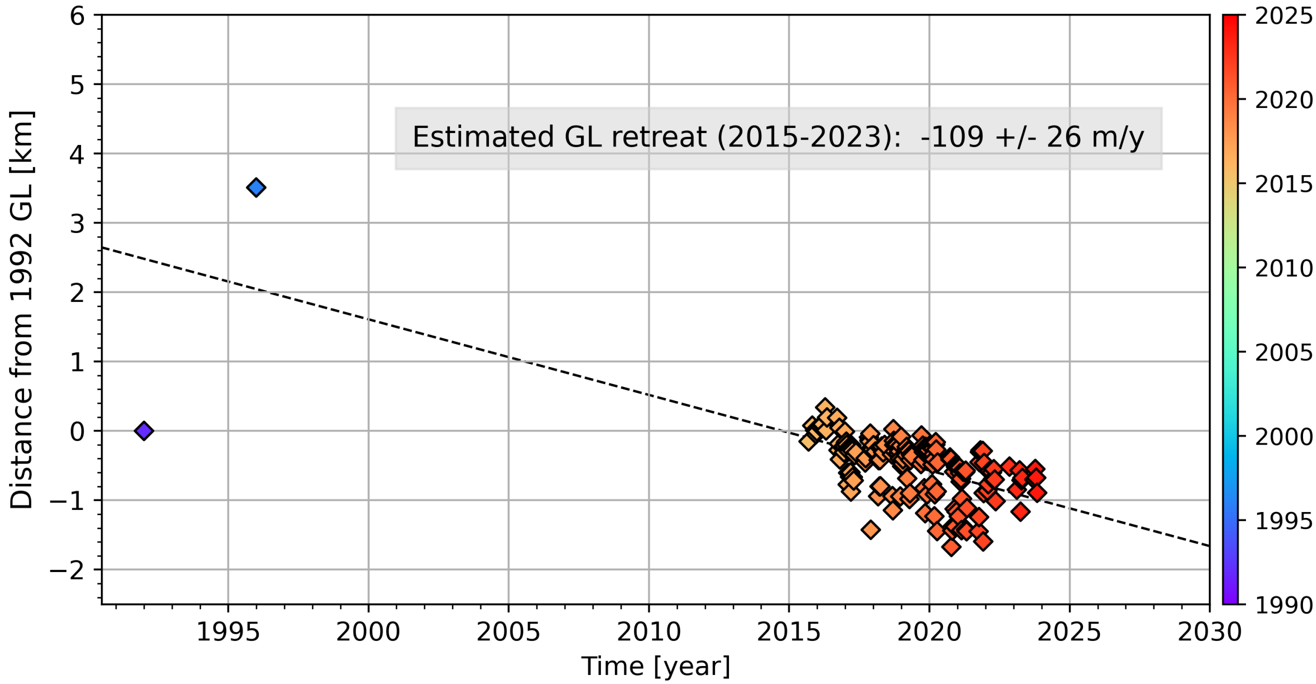

Figure S6. Time series of grounding line location for L. Bistrup (evaluated along the dashed transect in Figure 1). Grounding line locations are measured with double-difference interferometry using images from Sentinel-1 (2015-2024) and ERS-1/2 (1992-1996, data obtained from Mouginot et al. (2018)). Note that we exclude the 1992-1996 measurements from the linear fit, as L. Bistrup underwent a surge during this time. The short-term variability of the grounding line location is much higher for L. Bistrup than for Storstrømmen: the standard deviation of the de-trended grounding line location (excluding 1992-1996 data) is 338 m for L. Bistrup, compared to 119 m for Storstrømmen (see also Figure 1c in the main text for comparison).